Quantitative Finance, Vol. 12, No. 11, November 2012, 1679–1694

Options on realized variance by transform methods: a non-affine stochastic volatility model

GABRIEL G. DRIMUS*

Department of Mathematics, University of Copenhagen, Universitetsparken 5, DK-2100, Denmark

(*Received 15 October 2009; revised 17 April 2010; in final form 18 February 2011*)

In this paper we study the pricing and hedging of options on realized variance in the 3/2 non-affine stochastic volatility model by developing efficient transform-based pricing methods. This non-affine model gives prices of options on realized variance that allow upward-sloping implied volatility of variance smiles. Heston's model [*Rev. Financial Stud.*, 1993, **6**, 327–343], the benchmark affine stochastic volatility model, leads to downward-sloping volatility of variance smiles—in disagreement with variance markets in practice. Using control variates, we propose a robust method to express the Laplace transform of the variance call function in terms of the Laplace transform of the realized variance. The proposed method works in any model where the Laplace transform of realized variance is available in closed form. Additionally, we apply a new numerical Laplace inversion algorithm that gives fast and accurate prices for options on realized variance, simultaneously at a sequence of variance strikes. The method is also used to derive hedge ratios for options on variance with respect to variance swaps.

Keywords: Stochastic volatility; Volatility modelling; Computational finance; Derivatives pricing

JEL Classification: C6, C63, G1, G12, G13

1. Introduction

The trading and risk management of variance and volatility derivatives requires models that both adequately describe the stochastic behavior of volatility as well as allow for fast and accurate numerical implementation. This is especially important for variance markets since their underlying asset, namely the variance, displays much more volatility than the corresponding stock or index in the spot market. It is not uncommon for the volatility of variance to be several orders of magnitude higher than the volatility of the underlying stock or index. Many practical aspects relevant to variance and volatility markets are discussed by Bergomi (2005, 2008), Gatheral (2006) and Eberlein and Madan (2009).

Simple volatility derivatives, such as variance swaps, corridor variance swaps, gamma swaps and other similar variations, can be priced and hedged in a model-free way and hence do not require the specification of a stochastic volatility model. Neuberger (1994) made a first contribution to this area by proposing the use of the log contract as an instrument to hedge volatility risk. Due to their role in trading and hedging volatility, variance swaps have become liquidly traded instruments and have led to the development of other volatility derivatives. A comprehensive treatment of the model-free pricing and hedging of variance contracts can be found in Demeterfi *et al.* (1999), Carr and Madan (2002) and Friz and Gatheral (2005).

More complicated volatility derivatives, particularly options on realized variance and volatility, require explicit modeling of the dynamics of volatility. Important early stochastic volatility models studied in the literature include Scott (1987), Hull and White (1987) and Chesney and Scott (1989). Since no fast numerical methods are available to compute large sets of European option prices in these models, calibration procedures can become difficult. Heston (1993) proposed the use of an affine square root diffusion process to model the dynamics of instantaneous variance. The model has become widely popular due to its tractability and the existence of a closed-form expression for the characteristic function of log returns. The important result of Carr and Madan (1999) shows how to apply fast Fourier inversion

*Email: gdrimus@math.ku.dk

Quantitative Finance
ISSN 1469–7688 print/ISSN 1469–7696 online © 2012 Taylor & Francis
http://www.tandfonline.com
http://dx.doi.org/10.1080/14697688.2011.565789

techniques to price European options when the characteristic function is available in closed form.

The problem of pricing options on realized variance has received increasing attention in the recent literature. Broadie and Jain (2008a) and Sepp (2008) developed methods for pricing and hedging options on realized variance in the Heston model. Gatheral (2006) and Carr and Lee (2007) show how to use variance swap and volatility swap prices to fit a log-normal distribution to realized variance, thus arriving at Black–Scholes (1973) style formulas for prices and hedge ratios of options on variance. Several authors have considered the pricing of volatility derivatives in models with jumps. Carr *et al.* (2005) price options on realized variance by assuming the underlying asset follows a pure jump Sato process. Albanese *et al.* (2009) developed spectral methods for models of constant elasticity of variance (CEV) mixtures and Variance-Gamma (VG) jumps. Sepp (2008) augments the Heston dynamics with simultaneous jumps in returns and volatility and also considers the pricing of options on forward variance.

In this paper we determine and compare the prices and hedge ratios of options on realized variance in the 3/2 non-affine stochastic volatility model versus the Heston (1993) model. The 3/2 model has been used previously by Ahn and Gao (1999) to model the evolution of short interest rates, by Andreasen (2003) as a default intensity model in pricing credit derivatives, and by Lewis (2000) to price equity stock options. More recently, Carr and Sun (2007) have discussed the 3/2 model in the context of a new framework in which variance swap prices are modeled instead of the short variance process. Besides its analytical tractability, the 3/2 diffusion specification also enjoys empirical support in the equity market. Using S&P 100 implied volatilities, studies by Jones (2003) and Bakshi *et al.* (2006) estimate that the variance exponent should be around 1.3, which favors the 3/2 model over the 1/2 exponent in the Heston (1993) model. Additionally, as we show in this paper, the 3/2 and Heston models predict opposite dynamics for the short-term equity skew as a function of the level of short variance and, more importantly, the Heston model wrongly generates downward-sloping volatility of variance smiles, at odds with variance markets in practice.

We develop robust transform methods, based on control variates, to express the Laplace transform of the variance call function in terms of the Laplace transform of realized variance. Our approach works in any model where the Laplace transform of realized variance is available in closed form. We then apply a fast and accurate numerical Laplace inversion algorithm, recently proposed by Iseger (2006), which allows the use of the FFT technique of Cooley and Tukey (1965) to recover the variance call function at a sequence of strikes simultaneously. Finally, we show how these tools can be used to obtain hedge ratios for options on variance.

The paper is organized as follows. In section 2, we present general properties of the 3/2 and Heston models and compare them from the standpoint of short variance dynamics, equity skew dynamics and fitting to vanilla options. Section 3 is the main section, where we develop our transform methods and then apply them to pricing options on realized variance. In section 4, we discuss the derivation of hedge ratios with respect to variance swaps. Section 5 summarizes the main conclusions. All proofs not shown in the main text can be found in the appendix.

2. Model descriptions and properties

Two parametric stochastic volatility models are considered in this paper. The well-known Heston (1993) model assumes the following dynamics under the pricing measure $\mathbb{Q}$:

$$\frac{\mathrm{d}S_t}{S_t} = (r-\delta)\,\mathrm{d}t + \sqrt{v_t}\,\mathrm{d}B_t,$$
$$\mathrm{d}v_t = k(\theta - v_t)\,\mathrm{d}t + \epsilon\sqrt{v_t}\,\mathrm{d}W_t,$$

where r is the risk-free rate in the economy, δ is the dividend yield, and B_t and W_t are one-dimensional standard Brownian motions with correlation ρ. The parameters of the instantaneous variance diffusion have the usual meaning: k is the speed of mean reversion, θ is the mean reversion level and ϵ is the volatility of volatility. The theoretical results in this paper allow the mean reversion level to be time dependent, but deterministic. This can be useful if the model user wants to interpolate the entire term structure of variance swaps. Therefore, we allow the short variance process to obey the following extended Heston dynamics:

$$\mathrm{d}v_t = k(\theta(t) - v_t)\,\mathrm{d}t + \epsilon\sqrt{v_t}\,\mathrm{d}W_t, \tag{1}$$

where $\theta(t)$ is a time-dependent and deterministic function of time. An alternative model, which forms the main focus of our study, is known in the literature as the 3/2 model. It prescribes the following dynamics under the pricing measure $\mathbb{Q}$:

$$\frac{\mathrm{d}S_t}{S_t} = (r-\delta)\,\mathrm{d}t + \sqrt{v_t}\,\mathrm{d}B_t,$$
$$\mathrm{d}v_t = kv_t(\theta(t) - v_t)\,\mathrm{d}t + \epsilon v_t^{3/2}\,\mathrm{d}W_t, \tag{2}$$

where, as in the case of the extended Heston model, $\theta(t)$ is the time-dependent mean reversion level. However, it is important to note that the parameters k and ϵ no longer have the same interpretation and scaling as in the Heston model. The speed of mean reversion is now given by the product $k \cdot v_t$, which is a stochastic quantity; in particular, we see that variance will mean revert more quickly when it is high. Also, we should expect the parameter k in the 3/2 process to scale as $1/v_t$ relative to the parameter k in the Heston model; the same scaling applies to the parameter ϵ. These scaling considerations are useful when interpreting the parameter values obtained from model calibration.

We now address a couple of technical conditions needed to have a well-defined 3/2 model. An application of Itô's lemma to the process $1/v_t$ when v_t follows dynamics (2) gives

$$\mathrm{d}\left(\frac{1}{v_t}\right) = k\theta(t)\left(\frac{k+\epsilon^2}{k\theta(t)} - \frac{1}{v_t}\right)\mathrm{d}t - \frac{\epsilon}{\sqrt{v_t}}\,\mathrm{d}W_t,$$

which reveals that the reciprocal of the 3/2 short variance process is, in fact, a Heston process of parameters $(k\theta(t), (k+\epsilon^2)/k\theta(t), -\epsilon)$. Using Feller's boundary conditions, it is known that a time-homogeneous Heston process of dynamics (1), with $\theta(t)=\theta$, can reach the zero boundary with non-zero probability, unless

$$2k\theta \geq \epsilon^2.$$

This result has been extended by Schlögl and Schlögl (2000) to the case of time-dependent piecewise-constant Heston parameters. We have seen that, if v_t is a 3/2 process, then $1/v_t$ is a Heston process. A non-zero probability of reaching zero for $1/v_t$ would imply a non-zero probability for the short variance process to reach infinity. For a piecewise constant $\theta(t)$, applying the result of Schlögl and Schlögl (2000) to the dynamics of $1/v_t$, we obtain the non-explosion condition for the 3/2 process as

$$2k\theta(t)\cdot\frac{k+\epsilon^2}{k\theta(t)} \geq \epsilon^2,$$

or

$$k \geq -\frac{\epsilon^2}{2}. \tag{3}$$

In what follows we assume that $k>0$, which will automatically ensure that the non-explosion condition is satisfied. Another technical condition necessary in the 3/2 model refers to the martingale property of the process $S_t/\exp((r-\delta)t)$; Lewis (2000) shows that, for this process to be a true martingale, and not just a local martingale, the non-explosion test for (v_t) must be satisfied also under the measure that takes the asset price as numeraire. Applying the results of Lewis (2000) leads to the additional condition on the 3/2 model parameters

$$k - \epsilon\rho \geq -\frac{\epsilon^2}{2}. \tag{4}$$

If we require that the correlation parameter ρ be non-positive, this condition will be automatically satisfied. In practice, imposing the restriction $\rho \leq 0$ does not raise problems since the market behavior of prices and volatility usually displays negative correlation. To summarize, conditions (3) and (4) together ensure that we have a well-behaved 3/2 model. They are both satisfied if we impose the sufficient conditions $k>0$ and $\rho \leq 0$.

In this paper our focus will be on the pricing of options on *continuously sampled* realized variance, defined as the quadratic variation of the log-price process $\log(S_t)$. In both models considered—Heston (1993) and 3/2—we have, by Itô,

$$\mathrm{d}\log(S_t) = \left(r - \delta - \frac{v_t}{2}\right)\mathrm{d}t + \sqrt{v_t}\,\mathrm{d}B_t,$$

which shows that the annualized quadratic variation of $\log(S_t)$, hereafter denoted by V_T, is given by

$$V_T = \frac{1}{T}\int_0^T v_t\,\mathrm{d}t,$$

where T is the maturity of interest. In practice, volatility derivatives are written on the *discretely sampled* realized variance. Specifically, if we let $0=t_0<t_1<\cdots<t_N=T$ be a partition of $[0,T]$ with step size $t_i - t_{i-1} = \Delta$, the discretely sampled realized variance is calculated as

$$\frac{1}{T}\sum_{i=1}^{N}\log^2\left(\frac{S_{t_i}}{S_{t_{i-1}}}\right).$$

As the step size $\Delta \to 0$, the discretely sampled variance will converge to the continuously sampled variance. In practice, however, using the standard daily sampling frequency, non-negligible discrepancies arise in pricing options on realized variance with short maturities. The problem of discretely sampled variance is an important and large topic on its own; the reader is referred to Aït-Sahalia *et al.* (2005) and references therein as well as the recent study by Gatheral and Oomen (2010). Broadie and Jain (2008b) analyse the impact on realized variance of jumps and discrete sampling in standard models such as Merton (1976) and Heston (1993).

Of importance to our subsequent analysis will be the joint Fourier–Laplace transform of the log-price $X_T = \log(S_T)$ and the annualized variance $V_T = (1/T)\int_0^T v_t\,\mathrm{d}t$. In both models, it is possible to derive a closed-form solution for this joint transform. In particular, using the characteristic function of $X_T = \log(S_T)$ it is possible to price European options by Fourier inversion using the method developed by Carr and Madan (1999). Also, in the next section, we develop fast transform methods to price options on realized variance using the Laplace transform of V_T. Propositions 2.1 and 2.2 below give the expression for the joint transforms in the two models. Below, we let $X_t = \log(S_t e^{(r-\delta)(T-t)})$ denote the log-forward price process.

Proposition 2.1: *In the Heston model with time-dependent mean-reversion level, the joint conditional Fourier–Laplace transform of X_T and the de-annualized realized variance $\int_t^T v_s\,\mathrm{d}s$ is given by*

$$E\left(e^{iuX_T - \lambda\int_t^T v_s\,\mathrm{d}s} \mid X_t, v_t\right) = \exp(iuX_t + a(t,T) - b(t,T)v_t),$$

where

$$a(t,T) = -\int_t^T k\theta(s)b(s,T)\mathrm{d}s,$$
$$b(t,T) = \frac{(iu + u^2 + 2\lambda)(e^{\gamma(T-t)} - 1)}{(\gamma + k - i\epsilon\rho u)(e^{\gamma(T-t)} - 1) + 2\gamma},$$
$$\gamma = \sqrt{(k - i\epsilon\rho u)^2 + \epsilon^2(iu + u^2 + 2\lambda)}.$$

For the case when the mean-reversion level $\theta(t)$, $t \in [0,T]$, is a piecewise constant function it is possible to calculate explicitly the integral that defines $a(t,T)$

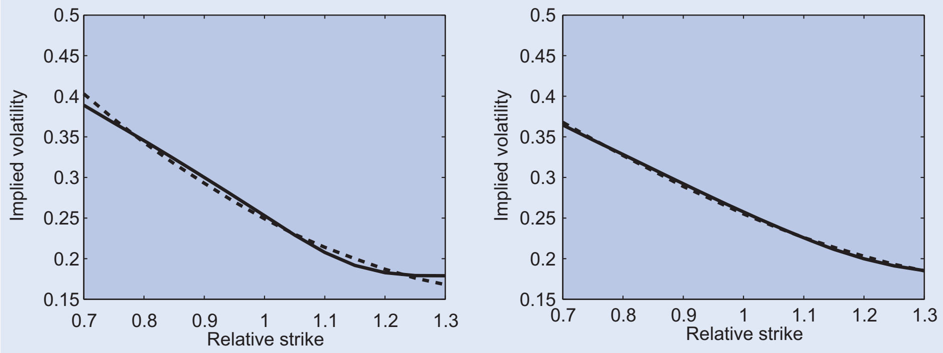

Figure 1. Simultaneous fit of the Heston model to 3-month (left) and 6-month (right) S&P 500 implied volatilities on July 31, 2009. (——) Heston implied volatilities. (--- -) Market implied volatilities. Heston parameters obtained: $v_0=25.56\%^2$, $k=3.8$, $\theta=30.95\%^2$, $\epsilon=92.88\%$ and $\rho=-78.29\%$.

in proposition 2.1. If we let $0=t_0<t_1<\cdots<t_N=T$ be a partition of $[0,T]$ such that $\theta(t)=\theta_j$ on the interval (t_j,t_{j+1}), $j\in\{0,1,2,\ldots,N-1\}$, then the function $a(t,T)$ is given by

$$a(t,T)=\sum_{j=0}^{N-1}\frac{k\theta_j}{\epsilon^2}\Bigg[(k-\gamma-i\epsilon\rho u)(t_{j+1}-t_j)\\ -2\log\left(\frac{\alpha e^{\gamma(T-t_{j+1})}+\beta e^{-\gamma(t_{j+1}-t_j)}}{\alpha e^{\gamma(T-t_{j+1})}+\beta}\right)\Bigg],$$

where

$$\alpha=\gamma+k-i\epsilon\rho u,$$
$$\beta=\gamma-k+i\epsilon\rho u,$$

with γ as defined in proposition 2.1. A similar result that gives the closed-form expression of the joint Fourier–Laplace transform can be obtained in the 3/2 model. The result is due to Carr and Sun (2007).

Proposition 2.2 (Carr and Sun 2007): *In the 3/2 model with time-dependent mean-reversion level, the joint conditional Fourier–Laplace transform of X_T and the de-annualized realized variance $\int_t^T v_s\,\mathrm{d}s$ is given by*

$$E\left(e^{iuX_T-\lambda\int_t^T v_s\,\mathrm{d}s}\mid X_t,v_t\right)\\ =e^{iuX_t}\frac{\Gamma(\gamma-\alpha)}{\Gamma(\gamma)}\left(\frac{2}{\epsilon^2 y(t,v_t)}\right)^{\alpha}M\left(\alpha,\gamma,\frac{-2}{\epsilon^2 y(t,v_t)}\right),$$

where

$$y(t,v_t)=v_t\int_t^T e^{\int_t^u k\theta(s)\mathrm{d}s}\,\mathrm{d}u,$$
$$\alpha=-\left(\frac{1}{2}-\frac{p}{\epsilon^2}\right)+\sqrt{\left(\frac{1}{2}-\frac{p}{\epsilon^2}\right)^2+2\frac{q}{\epsilon^2}},$$
$$\gamma=2\left(\alpha+1-\frac{p}{\epsilon^2}\right),$$
$$p=-k+i\epsilon\rho u,$$
$$q=\lambda+\frac{iu}{2}+\frac{u^2}{2},$$

and $M(\alpha,\gamma,z)$ is the confluent hypergeometric function, defined as

$$M(\alpha,\gamma,z)=\sum_{n=0}^{\infty}\frac{(\alpha)_n}{(\gamma)_n}\frac{z^n}{n!},$$

and

$$(x)_n=x(x+1)(x+2)\cdots(x+n-1).$$

Proof: We refer the reader to Carr and Sun (2007). □

Before looking at how the models differ in pricing exotic contracts, such as options on realized variance, we discuss, in the rest of this section, the pricing of European vanilla options. The calibration of the models to vanilla options is important because the prices of European options determine the values of variance swaps, which, in turn, are the main hedging instruments for options on realized variance; for a broad introduction to variance swaps we refer to Carr and Madan (2002). Moreover, vanilla options are also often used to hedge the vega exposure of options on realized variance.

We begin by fitting both models to market prices of S&P 500 European options; the fit is done simultaneously to two maturities: 3 months ($T=0.25$) and 6 months ($T=0.5$) on July 31, 2009.† In performing the calibration, we employ the FFT algorithm for European options developed by Carr and Madan (1999). The results are shown in figures 1 and 2. The parameters obtained are $(v_0,k,\theta,\epsilon,\rho):(25.56\%^2, 3.8, 30.95\%^2, 92.88\%, -78.29\%)$ in the Heston model and $(24.50\%^2, 22.84, 46.69\%^2, 8.56, -99.0\%)$ in the 3/2 model.

We remark that, while both models are able to fit the two maturities simultaneously, the Heston model parameters violate the non-zero boundary condition. This usually happens when calibrating the Heston model in equity markets; the empirical study of Bakshi *et al.* (1997) also finds Heston parameters that violate the non-zero boundary condition. This occurs because the Heston model requires a high volatility-of-volatility parameter ϵ to fit the steep skews in equity markets. On the other hand, the 3/2 parameters yield a well-behaved variance

†The data were kindly provided by an international investment bank.

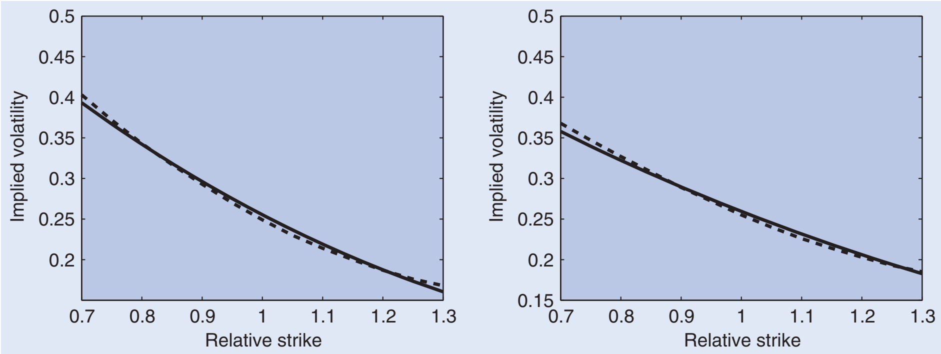

Figure 2. Simultaneous fit of the 3/2 model to 3-month (left) and 6-month (right) S&P 500 implied volatilities on July 31, 2009. (——) 3/2 implied volatilities. (--- -) Market implied volatilities. 3/2 parameters obtained: $v_0 = 24.50\%^2$, $k = 22.84$, $\theta = 46.69\%^2$, $\epsilon = 8.56$ and $\rho = -99.0\%$.

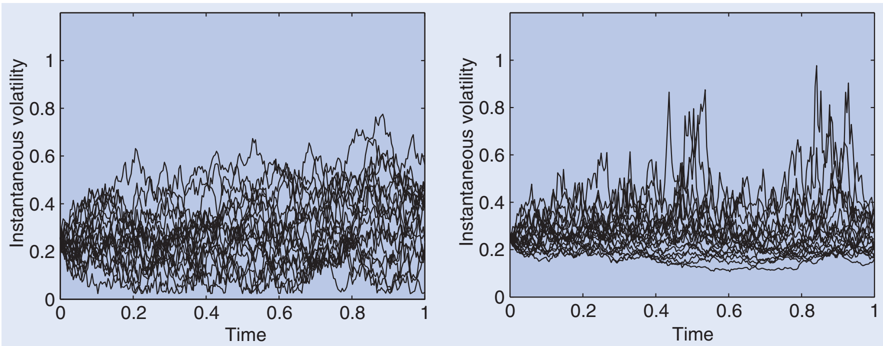

Figure 3. Instantaneous volatility (i.e. $\sqrt{v_t}$) paths in the Heston (left) and 3/2 model (right) using parameters calibrated to July 31, 2009 implied volatilities.

process that does not reach either zero or infinity. We note, however, that the 3/2 model requires a more negative correlation parameter (-99.0%) compared with the Heston model (-78.29%). We explain this by the much 'wilder' dynamics (also called 'dynamite dynamics' by Andreasen (2003)) of short variance in the 3/2 model—as illustrated in figure 3—which can cause a decorrelation with the spot process.

The modeling viewpoint of the 3/2 model as well as the modeling viewpoint of the Heston (1993) model can both be accommodated in the more general framework

$$\mathrm{d}v_t = (\alpha_0 + \alpha_1 v_t + \alpha_2 v_t^2 + \alpha_3 v_t^{-1})\mathrm{d}t + \beta_2 v_t^{\beta_3}\,\mathrm{d}W_t,$$

which was analysed in the econometric study of Bakshi *et al.* (2006). The authors use the square of the VIX index, sampled daily over a period of more than 10 years, as a proxy for the instantaneous variance process. Among the results of their statistical tests, the authors emphasize that "an overarching conclusion is that $\beta_3 > 1$ is needed to match the time-series properties of the VIX index" and find strong evidence rejecting the null hypothesis $\beta_3 \leq 1$. Indeed, the authors estimate a value of approximately 1.28 for the exponent β_3, which lends more support for the 1.5 exponent of the 3/2 model than the 0.5 exponent in the Heston (1993) model. The estimation for β_3 obtained by Bakshi *et al.* (2006) reinforces similar results from an earlier study by Jones (2003). Additionally, the study of Bakshi *et al.* (2006) finds evidence in favor of a nonlinear drift for the instantaneous variance diffusion. In particular, they find that the role of the quadratic term $\alpha_2 \cdot v_t^2$ is statistically more important than the linear term $\alpha_1 \cdot v_t$, thus rejecting a linear drift specification as in the Heston (1993) model; the authors find a significant $\alpha_2 < 0$ as in the quadratic drift of the 3/2 process.

Having noted the statistical evidence above, figure 3 also illustrates two qualitative differences between the evolution of instantaneous variance in the Heston model versus the 3/2 model: (a) the Heston variance paths spend much more time around the zero boundary and (b) the 3/2 model allows for the occurrence of extreme paths with short-term spikes in instantaneous volatility. From a trading and risk management perspective, both of these observations favor the 3/2 model. It is hard to justify a vanishing variance process and the non-existence of high (or extreme) volatility scenarios. In the 3/2 model, as indicated by the reversion speed $k \cdot v_t$, the process will revert faster towards the mean after short-term spikes in the instantaneous variance. Figure 3(right) illustrates this behavior graphically. We remark that short-term market volatility, as reflected, for example, by CBOE's VIX index, exhibits similar short-term spikes during periods of market stress. In the next section we see that these differences have a major effect on the prices of options on realized variance.

Another important difference is in the behavior of implied volatility smiles. Specifically, the steepness of the smile responds in opposite ways to changes in the level of short variance in the two models. To show this, we make use of the implied volatility expansion derived by Medvedev and Scailett (2007) for short times to expiration and near the money options. Letting $X=\log(K/S_0 e^{(r-\delta)T})$ denote the log-forward-moneyness corresponding to a European option with strike K and maturity T, we apply proposition 1 of Medvedev and Scaillet (2007) to the case of the Heston and 3/2 models. One obtains the following expansions for implied volatility $I(X,T)$ in the neighborhood of $X=T=0$. For the Heston model:

$$I(X,T)=\sqrt{v_0}+\frac{\rho\epsilon X}{4\sqrt{v_0}}+\left(1-\frac{5\rho^2}{2}\right)\frac{\epsilon^2 X^2}{24 v_0^{3/2}} + \left(\frac{k(\theta-v_0)}{4\sqrt{v_0}}+\frac{\rho\epsilon\sqrt{v_0}}{8}+\frac{\rho^2\epsilon^2}{96\sqrt{v_0}}-\frac{\epsilon^2}{24\sqrt{v_0}}\right)T+\cdots,$$

which gives the at-the-money-forward skew

$$\left.\frac{\partial I}{\partial X}(X,T)\right|_{X=0}=\frac{\rho\epsilon}{4\sqrt{v_0}},\quad T\to 0.$$

And for the 3/2 model:

$$I(X,T)=\sqrt{v_0}+\frac{\rho\epsilon\sqrt{v_0}X}{4}+\left(1-\frac{\rho^2}{2}\right)\frac{\epsilon^2\sqrt{v_0}X^2}{24} + \left(\frac{k(\theta-v_0)}{4}+\frac{\rho\epsilon v_0}{8}-\frac{7\rho^2\epsilon^2 v_0}{96}-\frac{\epsilon^2 v_0}{24}\right)\sqrt{v_0}T+\cdots,$$

which gives the at-the-money-forward skew

$$\left.\frac{\partial I}{\partial X}(X,T)\right|_{X=0}=\frac{\rho\epsilon\sqrt{v_0}}{4},\quad T\to 0.$$

From figure 4 we see very good agreement between the Medvedev and Scaillet (2007) expansion and the true implied volatilities calculated by Fourier inversion. Since the expansions are valid only for short expirations and close to the money, we chose a one month maturity and a [90%, 110%] relative strike range. Therefore, in the Heston model, the short-term skew flattens when the instantaneous variance increases, whereas in the 3/2 model the short-term skew steepens when the instantaneous variance increases. It is important to realize that this implies very different dynamics for the evolution of the implied volatility surface. The Heston model predicts that, in periods of market stress, when the instantaneous volatility increases, the skew will flatten. Under the same scenario, the skew will steepen in the 3/2 model. From a trading and risk management perspective, since the magnitude of the skew is itself a measure of market stress, the behavior predicted by the 3/2 model appears more credible.

3. Transform pricing of options on realized variance

The main quantity of interest in pricing options on realized variance is the annualized integrated variance, given by

$$V_T=\frac{1}{T}\int_0^T v_t\,\mathrm{d}t.$$

We study the prices of call options on realized variance; prices of put options follow by put–call parity. The payoff of a call option on realized variance with strike K and maturity T is defined as

$$\left(\frac{1}{T}\int_0^T v_t\,\mathrm{d}t-K\right)_+=(V_T-K)_+.$$

In a key result, Carr and Madan (1999) showed that, starting from the characteristic function of the log stock price $\log(S_T)$, it is possible to derive a closed-form expression for the Fourier transform of the (dampened) call price viewed as a function of the log strike $k=\log(K)$. Once the call price transform is known, fast inversion algorithms—such as the FFT method developed by Cooley and Tukey (1965)—can be applied to recover the call prices at a sequence of strikes simultaneously. This technique is now widely used in the literature to price stock options in non-Black–Scholes models that have closed-form expressions for the characteristic function of $\log(S_T)$. We now develop a similar idea for the problem of pricing options on realized variance. Specifically, we show that, starting from the Laplace transform of integrated

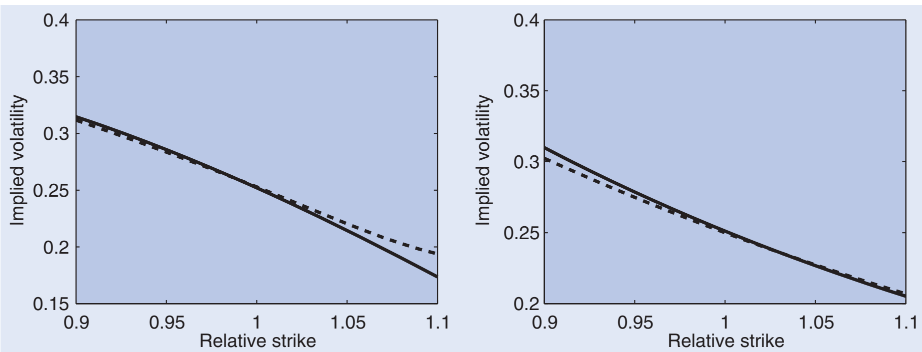

Figure 4. Comparison between true model implied volatilities and the Medvedev and Scaillet (2007) expansion for a maturity of one month. Left: Heston model. Right: 3/2 model. (——) Medvedev and Scaillet (2007) approximation. (- - - -) True model implied volatilities.

variance, it is possible to derive, in closed form, the Laplace transform of the variance call price viewed as a function of the variance strike. This idea was first suggested by Carr *et al.* (2005). After providing a proof, we propose an important improvement of the result by the use of control variates. Additionally, we demonstrate the application of a new numerical Laplace inversion algorithm that gives prices of options on realized variance for a sequence of variance strikes simultaneously.

Proposition 3.1: *Let $\mathcal{L}(\cdot)$ denote the Laplace transform of the annualized realized variance over* $[0, T]$:

$$\mathcal{L}(\lambda) = E\left(\mathrm{e}^{-\lambda(1/T)\int_0^T v_t\,\mathrm{d}t}\right).$$

Then the undiscounted variance call function $C:[0,\infty)\to\mathbb{R}$, *defined by*

$$C(K) = E\left(\frac{1}{T}\int_0^T v_t\,\mathrm{d}t - K\right)_+,$$

has Laplace transform given by

$$L(\lambda) = \int_0^\infty \mathrm{e}^{-\lambda K} C(K)\mathrm{d}K = \frac{\mathcal{L}(\lambda)-1}{\lambda^2} + \frac{C(0)}{\lambda}. \qquad (5)$$

Proof: Let $\mu(\mathrm{d}x)$ denote the probability law of the annualized realized variance $(1/T)\int_0^T v_t\,\mathrm{d}t$. We have to compute

$$L(\lambda) = \int_0^\infty \mathrm{e}^{-\lambda K}\int_K^\infty (x-K)\mu(\mathrm{d}x)\mathrm{d}K.$$

Since the integrand in this double integral is non-negative, we can apply Fubini's theorem to change the order of integration, and we obtain

$$\int_0^\infty\int_0^x \mathrm{e}^{-\lambda K}(x-K)\mathrm{d}K\mu(\mathrm{d}x).$$

The inner integral now follows readily by integration by parts

$$\int_0^x \mathrm{e}^{-\lambda K}(x-K)\mathrm{d}K = \frac{\mathrm{e}^{-\lambda x}-1}{\lambda^2} + \frac{x}{\lambda}.$$

Finally, we can compute the Laplace transform as follows:

$$L(\lambda) = \int_0^\infty\left(\frac{\mathrm{e}^{-\lambda x}-1}{\lambda^2}+\frac{x}{\lambda}\right)\mu(\mathrm{d}x) = \frac{\mathcal{L}(\lambda)-1}{\lambda^2}+\frac{C(0)}{\lambda},$$

where we have used

$$C(0) = E\left(\frac{1}{T}\int_0^T v_t\,\mathrm{d}t\right).$$

□

Relation (5) of proposition 3.1 gives a closed-form solution for the Laplace transform $L(\lambda)$ of the variance call function $C(K)$ in terms of the Laplace transform $\mathcal{L}(\lambda)$ of the annualized realized variance $V_T = (1/T)\int_0^T v_t\,\mathrm{d}t$. The closed-form expression for $\mathcal{L}(\lambda)$ is obtained from propositions 2.1 and 2.2 by setting $t=0$, $u=0$ and $\lambda=\lambda/T$.

However, we note that the following two polynomially decaying terms appear in expression (5):

$$\frac{-1}{\lambda^2}+\frac{C(0)}{\lambda}.$$

These vanish slowly as $|\lambda|\to\infty$, affecting the accuracy of numerical inversion algorithms. The term $C(0)/\lambda$ appears because the function has a discontinuity of size $C(0)$ at 0, while the term $-1/\lambda^2$ appears because the first derivative has a discontinuity of size -1 at 0 (as shown below). We propose to eliminate these slowly decaying terms by applying the idea of control variates. Specifically, we choose a proxy distribution for the realized variance that allows the calculation of the variance call function in closed form. Denote this control variate function by $\tilde{C}(\cdot)$. If we choose the proxy distribution such that it has the same mean as the true distribution of realized variance, we have $C(0)=\tilde{C}(0)$. Then, by the linearity of the Laplace transform we obtain

$$L_{C-\tilde{C}}(\lambda) = L_C(\lambda) - L_{\tilde{C}}(\lambda) = \frac{\mathcal{L}(\lambda)-\tilde{\mathcal{L}}(\lambda)}{\lambda^2}.$$

Both power terms have been eliminated since the difference $C(\cdot)-\tilde{C}(\cdot)$ is now a function that is both continuous and differentiable at zero. Differentiability comes from the fact that both functions have a right derivative at 0 equal to -1. This is seen from the following simple lemma.

Lemma 3.2: *Let V be a random variable such that $V>0$ a.s. and $E(V)<\infty$. Then the function $C:[0,\infty)\to\mathbb{R}$, defined by*

$$C(K) = E(V-K)_+,$$

satisfies

$$\lim_{K\downarrow 0}\frac{C(K)-C(0)}{K} = -1.$$

In summary, by making use of a control variate we can achieve smooth pasting at 0. In choosing the proxy distribution for realized variance, one appealing choice is the log-normal distribution. This would give Black–Scholes style formulas for the control variate function $\tilde{C}(\cdot)$. However, this choice does not work because the Laplace transform of the log-normal distribution is not available in closed form. Instead, we choose the Gamma distribution as our proxy distribution. The Laplace transform is known in closed form and the following lemma shows how to compute the control variate function $\tilde{C}(\cdot)$.

Lemma 3.3: *Let the (annualized) realized variance over $[0, T]$ follow a Gamma distribution of parameters (α,β). Specifically, assume the density of realized variance is*

$$\frac{1}{\Gamma(\alpha)\beta^\alpha}x^{\alpha-1}\mathrm{e}^{-x/\beta}, \quad x>0.$$

Then the control variate function $\tilde{C}(\cdot)$ is given by

$$\tilde{C}(K) = \alpha\beta(1-F(K;\alpha+1,\beta)) - K(1-F(K;\alpha,\beta)),$$

where $F(x;\alpha,\beta)$ *is the Gamma cumulative distribution function of parameters* (α,β).

To ensure that $\tilde{C}(0)=C(0)$, the only necessary condition on α and β is that the mean of the Gamma distribution matches $C(0)$:

$$\alpha\beta = C(0).$$

Since we have two parameters, from a theoretical standpoint we can choose one of them freely. Optionally, the extra parameter could be used to fix the second moment of the proxy distribution. For example, we can match the second moment of the model realized variance:

$$\alpha\beta^2+(\alpha\beta)^2 = E\left(\frac{1}{T}\int_0^T v_t\,\mathrm{d}t\right)^2 = \frac{\partial^2\mathcal{L}}{\partial\lambda^2}(\lambda)\bigg|_{\lambda=0},$$

where $\mathcal{L}(\cdot)$ is the Laplace transform of realized variance. In the Heston model, the second moment of realized variance is available in closed form (Dufresne 2001). In the 3/2 model, however, we do not have a closed-form formula for the second moment of realized variance; as shown below, even the calculation of the first moment requires the development of some additional results. In this case, the second moment could be approximated by using a finite difference for the second derivative of $\mathcal{L}(\cdot)$ at zero. Alternatively, an easier approach to choose a reasonable second moment for the control variate distribution is to match the second moment of a log-normal distribution of the form

$$C(0)\mathrm{e}^{\sigma\sqrt{T}N(0,\,1)-(\sigma^2T/2)},$$

where $N(0,\,1)$ is a standard normal random variable and σ is a parameter of our choice—a sensible choice would have an order of magnitude that is representative for the implied volatility of variance. As the subsequent numerical results reveal, any choice for σ in the range of, say, [50%, 150%] would be reasonable. The second moment condition on α and β reads

$$\alpha\beta^2+(\alpha\beta)^2 = C(0)^2\mathrm{e}^{\sigma^2T}.$$

We obtain that a possible choice for the parameters of the proxy distribution is

$$\alpha = \frac{C(0)}{\beta},$$
$$\beta = C(0)(\mathrm{e}^{\sigma^2T}-1).$$

To implement the above calculations, one needs to be able to determine

$$E\left(\int_0^T v_t\,\mathrm{d}t\right)$$

in both models—Heston and 3/2. The computation is straightforward in the Heston model, but is more complicated in the 3/2 model. We first show the calculation for the Heston model with a piecewise constant mean-reversion level $\theta(t)$, $t\in[0,T]$. If we let $\theta(t)=\theta_i$ on (t_i,t_{i+1}), $i\in\{0,1,2,\ldots,N-1\}$, we can write

$$E\left(\int_0^T v_t\,\mathrm{d}t\right) = \sum_{i=0}^{N-1}E\left(\int_{t_i}^{t_{i+1}} v_t\,\mathrm{d}t\right),$$

where

$$E\left(\int_{t_i}^{t_{i+1}} v_t\,\mathrm{d}t\right) = \frac{\mathrm{e}^{-kt_i}-\mathrm{e}^{-kt_{i+1}}}{k}\cdot\left(v_0+\sum_{j=0}^{i-1}\theta_j\,(\mathrm{e}^{kt_{j+1}}-\mathrm{e}^{kt_j})\right) + \frac{\theta_i}{k}(\mathrm{e}^{-k(t_{i+1}-t_i)}-1+k(t_{i+1}-t_i)).$$

In the case of the 3/2 model, Carr and Sun (2007, theorem 4) show that

$$E\left(\int_0^T v_t\,\mathrm{d}t\right) = h\left(v_0\int_0^T \mathrm{e}^{k\int_0^t\theta(s)\mathrm{d}s}\,\mathrm{d}t\right),$$

where

$$h(y) = \int_0^y \mathrm{e}^{-2/\epsilon^2 z}\cdot z^{2k/\epsilon^2}\cdot\int_z^\infty \frac{2}{\epsilon^2}\mathrm{e}^{2/\epsilon^2 u}u^{(-2k/\epsilon^2)-2}\,\mathrm{d}u\,\mathrm{d}z. \tag{6}$$

The integral appearing in the argument to the function $h(\cdot)$ is straightforward to compute for a piecewise constant $\theta(t)$:

$$\int_0^T \mathrm{e}^{k\int_0^t\theta(s)\mathrm{d}s}\,\mathrm{d}t = \sum_{i=0}^{N-1}\int_{t_i}^{t_{i+1}}\mathrm{e}^{k\int_0^t\theta(s)\mathrm{d}s}\,\mathrm{d}t,$$

where

$$\int_{t_i}^{t_{i+1}}\mathrm{e}^{k\int_0^t\theta(s)\mathrm{d}s}\,\mathrm{d}t = \frac{\mathrm{e}^{k\theta_i(t_{i+1}-t_i)}-1}{k\theta_i}\cdot\exp\left(k\sum_{j=0}^{i-1}\theta_j\,(t_{j+1}-t_j)\right).$$

However, the integral representation (6) of the function $h(\cdot)$ is hard to use for fast and accurate numerical implementations. We prove an alternative representation based on a uniformly convergent series whose terms are easy to calculate and the total error can be controlled *a priori*. The result is formulated in proposition 3.4 and lemma 3.5.

Proposition 3.4: *The function* $h(\cdot)$ *admits the following uniformly convergent series representation*:

$$h(y) = \alpha\cdot\left(\frac{E(\alpha/y)}{1-\beta}+\sum_{n=1}^\infty\frac{F_{\alpha/y}(n)}{n(n-\beta+1)}\right),$$

where

$$E(x) = \int_x^\infty \mathrm{e}^{-t}\cdot t^{-1}\,\mathrm{d}t,\quad x>0,$$
$$F_\nu(n) = P(Z\le n),\quad Z\sim\mathrm{Poisson}(\nu),$$
$$\alpha = \frac{2}{\epsilon^2},$$
$$\beta = \frac{-2k}{\epsilon^2}.$$

In proposition 3.4 we recognize the special function $E(x)$ as the exponential integral that is readily accessible in any numerical package. The terms appearing in the infinite series are very fast and easy to compute. Moreover, as shown in lemma 3.5 below, the total error arising from truncating the series can be controlled *a priori*.

Lemma 3.5: *The infinite series of proposition* 3.4 *has a remainder term*

$$R_k = \sum_{n=k}^{\infty} \frac{F_{\alpha/y}(n)}{n(n-\beta+1)},$$

which is positive and satisfies the following bounds:

$$\frac{F_{\alpha/y}(k)}{m+1}\left(\frac{1}{k}+\frac{1}{k+1}+\cdots+\frac{1}{k+m}\right) < R_k < \frac{1}{k},$$

where $m = \lceil -\beta \rceil$. *If we let* $\bar{R}$ *be the mid-point between the two bounds, i.e.*

$$\bar{R} = \frac{1}{2}\left(\frac{1}{k}+\frac{F_{\alpha/y}(k)}{m+1}\left(\frac{1}{k}+\frac{1}{k+1}+\cdots+\frac{1}{k+m}\right)\right),$$

then we also have

$$|R_k - \bar{R}| < \frac{m+(\alpha/y)}{4k^2}. \tag{7}$$

The application of lemma 3.5 proceeds as follows. To compute $h(y)$, for a given y, use bound (7) to determine the number of terms needed to achieve the desired precision and then set

$$h(y) \approx \alpha \cdot \left(\frac{E(\alpha/y)}{1-\beta} + \sum_{n=1}^{k-1} \frac{F_{\alpha/y}(n)}{n(n-\beta+1)} + \bar{R}\right).$$

Having completed our discussion concerning the determination of the Laplace transform of the variance call function, we now turn to the problem of choosing a fast and accurate Laplace inversion algorithm. Many numerical Laplace inversion algorithms have been proposed in the literature; some important early contributions in this area include Weeks (1966), Dubner and Abate (1968), Stehfest (1970), Talbot (1979) and Abate and Whitt (1992). In what follows, we apply the very efficient algorithm recently proposed by Iseger (2006). Extensive analysis and numerical tests indicate that this algorithm is faster and more accurate than the other methods available. For a detailed treatment of the numerical and mathematical properties of this new method we refer the reader to Iseger (2006). We now outline the main steps of the method.

Suppose we want to recover the difference between the variance call functions $C - \tilde{C}$ at a sequence of variance strikes $k\Delta$, $k = 0, 1, \ldots, M-1$. Let $g(k) = C(k\Delta) - \tilde{C}(k\Delta)$ and $\hat{g}$ be the Laplace transform of g. The starting point of the method is the well-known Poisson summation formula, which states that, for any $v \in [0, 1)$, the following identity holds for the function g:

$$\sum_{k=-\infty}^{\infty} \hat{g}(a + 2\pi i(k+v)) = \sum_{k=0}^{\infty} e^{-ak} e^{-2\pi i k v} g(k), \tag{8}$$

where a is a positive damping factor. The Poisson summation formula applies to functions of bounded variation and in $L^1[0,\infty)$. To check these conditions for the function g, we derive the simple lemma 3.6.

Lemma 3.6: *Let* V *be a random variable such that* $V > 0$ *a.s. and* $E(V^2) < \infty$. *Then the function* $C: [0,\infty) \to \mathbb{R}$, *defined by*

$$C(K) = E(V-K)_+,$$

belongs to $L^1[0,\infty)$ *and is of bounded variation.*

In both the Heston and the 3/2 model, the Laplace transform of integrated variance exists in the neighborhood of zero, which implies that all moments of integrated variance are finite. The same is true for our control variate distribution, Gamma. Applying lemma 3.6, we conclude that functions $C(\cdot)$ and $\tilde{C}(\cdot)$ are in $L^1[0,\infty)$ and are of bounded variation. It follows that the function g satisfies the same conditions.

Equation (8) relates an infinite sum of Laplace transform values (the LHS) to a dampened series of function values (the RHS). This result also forms the basis of the method developed by Abate and Whitt (1992). The series of Laplace transform values usually converges slowly and Abate and Whitt (1992) proposed a technique, known as Euler summation, to increase the rate of convergence for this series. Iseger (2006) proposed a completely different idea for handling the infinite series of Laplace transform values. It constructs a Gaussian quadrature rule for the series on the LHS of (8). Specifically, the infinite sum is approximated by a finite sum of the form

$$\sum_{k=1}^{n} \beta_k \cdot \hat{g}(a + i\lambda_k + 2\pi i v),$$

where β_k are the quadrature weights and λ_k the quadrature points. The exact numbers β_k and λ_k can be found in Iseger (2006, appendix A) for various values of n. It is found that $n = 16$ quadrature points is sufficient for results attaining machine precision.

Having developed a fast and accurate approximation for the LHS of (8), we now turn to the dampened series of function values on the RHS. This series is much easier to handle. As shown by Iseger (2006) it is possible to choose the damping parameter a and a truncation rank M_2 to attain any desired level of truncation error. For double precision, the authors recommend truncating the series after $M_2 = 8M$ terms and using a dampening factor $a = 44/M_2$. Finally, applying the identity (8) repeatedly for all $v \in \{0, 1/M_2, 2/M_2, \ldots, (M_2-1)/M_2\}$, we can recover each function value $g(k)$ by inverting the discrete Fourier series on the RHS as follows:

$$\frac{e^{ak}}{M_2} \cdot \sum_{j=0}^{M_2-1} \left[e^{2\pi i k(j/M_2)} \sum_{l=1}^{n} \beta_l \cdot \hat{g}\left(a + i\lambda_l + 2\pi i \frac{j}{M_2}\right)\right]. \tag{9}$$

An important advantage of this method is that these sums can all be calculated simultaneously for all $k \in \{0, 1, 2, \ldots, M_2 - 1\}$ using the FFT algorithm of Cooley and Tukey (1965). In the end, we retain the first M values in

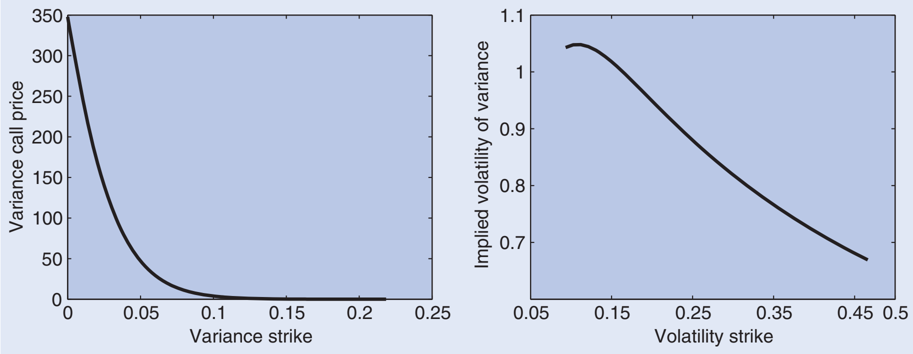

Figure 5. Left: Variance call prices as a function of variance strike using Heston parameters from Bakshi *et al.* (1997) and a maturity of 6 months. Right: Implied volatility of variance as a function of volatility strike.

which we are interested. For the FFT algorithm it is recommended that M be a power of 2. In the rest of the paper, we shall refer to the Iseger (2006) numerical inversion algorithm as the Gaussian-Quadrature-FFT algorithm or *GQ-FFT*.

As an application of the tools developed so far, we now price options on realized variance in the Heston and 3/2 models. Similar to options on stocks, market practitioners express the prices of realized variance options in terms of Black–Scholes implied volatilities. Specifically, the undiscounted variance call price obtained from the model—Heston or 3/2, in our case—is matched to a Black–Scholes formula with zero rate and zero dividend yield:

$$C(K) = C(0)N(d_1) - KN(d_2),$$

where $C(0) = E((1/T)\int_0^T v_t\,\mathrm{d}t)$ is the fair variance as seen at time 0, and

$$d_1 = \frac{\log(C(0)/K) + (\xi^2 T/2)}{\xi\sqrt{T}},$$
$$d_2 = d_1 - \xi\sqrt{T}$$

are the usual Black–Scholes terms. The parameter ξ, ensuring the equality between the model price and the Black–Scholes price, will be called the implied *volatility of variance*, corresponding to strike K.

As a simple first numerical example, we take a standard choice for the Heston parameters from the existing literature. In an empirical investigation, Bakshi *et al.* (1997) estimated the following parameter set for the Heston model: $v_0 = 0.0348$, $k = 1.15$, $\theta = 0.0348$, and $\varepsilon = 0.39$. Gatheral (2006) also uses the parameter set of Bakshi *et al.* (1997) to analyse prices of options on realized variance.† Here we apply our previous Laplace transform techniques to determine the prices of call options on 6-month realized variance. Figure 5(left) shows the (undiscounted) variance call function recovered over a wide strike range, from $K = 0$ to $K = 0.48^2$; the call prices have been scaled by a notional of 10 000. A single run of the GQ-FFT algorithm computes the variance call prices for the entire sequence of strikes considered. As mentioned earlier, it is natural to convert these absolute prices into implied volatilities of variance. Figure 5(right) shows the implied volatilities of variance as a function of strike expressed as a volatility.

Compared with the spot market, we see that volatilities of variance can be several orders of magnitude higher than the volatility of the underlying stock or index. Depending on the volatility strike and maturity, it is common to see volatilities of variance in the range [50%, 150%]. For short maturities, the implied volatilities of variance increase very quickly; this makes trading sense, since the shorter the period, the more uncertainty about the future realized variance. We refer the reader to Bergomi (2005, 2008) where many practical aspects of volatility markets are discussed. Figure 5 also reveals the main drawback of pricing volatility derivatives in the Heston model. We obtain a downward-sloping smile for the volatility of variance, whereas the slope is strongly positive in practice (see, for example, Bergomi (2008)). From a trading and risk management perspective, it is clear that upside calls on variance should be more expensive, since during periods of market stress when the volatility is high, the volatility of volatility is also very high. This behavior cannot be captured by the Heston model.

Figure 6 shows the implied volatilities of variance in the Heston versus the 3/2 model, with the parameters calibrated in the previous section. We price 3-month and 6-month options on realized variance. Note that, in both models, the volatilities are higher for 3-month variance than for 6-month variance; this is in line with our expectation. Most importantly, figure 6 shows that, unlike the Heston model, the 3/2 model generates upward-sloping volatility of variance smiles, thus capturing an important feature of the volatility derivatives market.

To further investigate the differences between the Heston and 3/2 models, we compare the densities of realized variance. Since the GQ-FFT algorithm gives us the variance call function for a sequence of strikes simultaneously, we can apply the well-known Breeden and Litzenberger (1978) formula to obtain the density of realized variance as follows:

$$\phi_{\mathrm{RV}}(K) = \frac{\partial^2}{\partial K^2} C(K).$$

†Note that Gatheral(2006) uses slightly modified values for v_0 and θ.

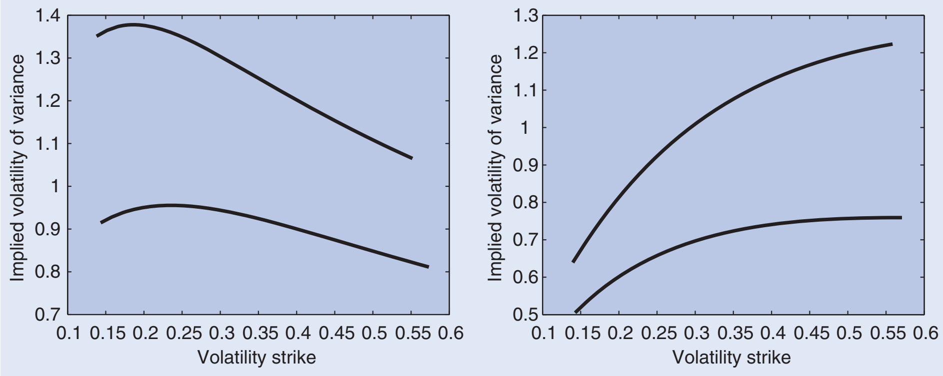

Figure 6. Implied volatility of variance as a function of volatility strike. Left: Heston model. Right: 3/2 model. Maturities of 3 months (top curve) and 6 months (bottom curve).

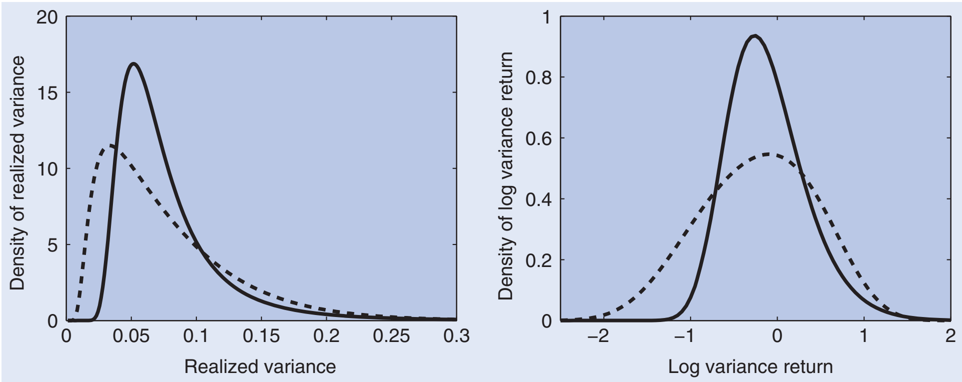

Figure 7. Left: Densities of 3-month realized variance. Right: Densities of 3-month log realized variance return. (——) 3/2 model. (- - - -) Heston model.

Applying this formula, we obtain in figure 7(left) the densities of the 3-month realized variance in the Heston and 3/2 models. We see that the well-behaved and accurate prices obtained by our Laplace methods allow us to obtain a smooth and positive density for a wide range of variance values (in this case, from $K=0$ to $K=55\%^2$). We note that the 3/2 density is much more peaked and places less weight for variance near zero. In equity markets, the Heston fits often violate the zero boundary test, thus assigning significant probabilities to low variance scenarios. To better explain the downward/upward-sloping volatility of variance smiles, we plot, in figure 7(right), the density of the log realized variance return:

$$\log\left(\frac{(1/T)\int_0^T v_t\,\mathrm{d}t}{C(0)}\right),$$

which we obtain from the density of the realized variance $(1/T)\int_0^T v_t\,\mathrm{d}t$ as follows:

$$\phi_{\mathrm{LogRV}}(k) = C(0)\cdot \mathrm{e}^k \cdot \phi_{\mathrm{RV}}(C(0)\mathrm{e}^k).$$

We note from figure 7(right) that, in the Heston model, the variance log return is skewed to the left, whereas in the 3/2 model the variance log return is skewed to the right. This explains why the variance smile is downward sloping in the Heston model and upward sloping in the 3/2 model.

We conclude this section with a detailed explanation of the key advantages of our pricing method for options on realized variance compared with a direct application of the standard Fourier methods from the literature. As will be seen below, recovering the variance call function $C(K)$ can, indeed, be easily written in terms of Fourier inversion. Specifically, since in both models—Heston (1993) and 3/2—the Laplace transform $L(\lambda)$ of the variance call function $C(K)$ is well defined in the entire half-plane, for any $a \geq 0$ fixed we can write

$$\begin{aligned} L(a+iu) &= \int_0^\infty \mathrm{e}^{-iuK}\cdot \mathrm{e}^{-aK} C(K)\mathrm{d}K \\ &= \mathcal{F}\{\mathrm{e}^{-aK}\cdot 1_{K\geq 0}\cdot C(K)\}(u), \end{aligned}$$

where $u \in \mathbb{R}$ and $\mathcal{F}\{\cdot\}$ denotes the Fourier transform. Applying Fourier inversion, we can recover the variance call function at any strike $K \geq 0$ by

$$C(K) = \frac{\mathrm{e}^{aK}}{2\pi}\int_{-\infty}^\infty \mathrm{e}^{iuK} L(a+iu)\mathrm{d}u.$$

As in Carr and Madan (1999), since the function $C(K)$ is real, this can be written equivalently as

$$C(K) = \frac{\mathrm{e}^{aK}}{\pi}\,\mathrm{Re}\left\{\int_0^\infty \mathrm{e}^{iuK} L(a+iu)\mathrm{d}u\right\} \tag{10}$$

Hence, from a mathematical standpoint, the problem becomes identical to that of European vanilla options as treated by Carr and Madan (1999). The next step in the standard Fourier method is the truncation and then the discretization of the integral in (10). However, a key difference arising in our case is the singularity of the call function $C(K)$ at zero, which will cause the oscillations in the integrand $e^{iuK} L(a+iu)$ to decay slowly as $u \to \infty$, thus making the truncation of the integral a highly heuristic and unstable exercise. This singularity problem is circumvented in the case of European vanilla options by changing the variable from absolute strikes K to log-strikes $k = \log K$ and thus 'pushing' the singularity to $-\infty$. Suppose we tried to follow the same idea for variance call options and define

$$c(k) = E\left(\frac{1}{T}\int_0^T v_t \, \mathrm{d}t - \mathrm{e}^k\right)_+,$$

as in the standard method for European vanilla options. Taking $a \geq 0$ such that $\mathrm{e}^{ak}c(k)$ is integrable on $\mathbb{R}$, the main result of Carr and Madan (1999) would give us a closed-form relation between the Fourier transform of $\mathrm{e}^{ak}c(k)$ and the Fourier transform of log-realized variance $\log((1/T)\int_0^T v_t \, \mathrm{d}t)$. However, in both the Heston (1993) model and the 3/2 model, the Fourier transform of log-realized variance is not available in closed form. We have closed-form expressions for the Fourier transform of realized variance, but not for the log-realized variance. Therefore, a direct application of the standard Fourier methods of Carr and Madan (1999) will not be possible for options on realized variance.

Nevertheless, if we proceed by truncating the integral in (10), the truncation problem can be significantly alleviated by applying the idea of control variates. As can be seen from figure 8, the integrand will decay much faster, making the truncation more stable. In our opinion, for options on realized variance, it is not possible to robustly truncate the integral in (10) without control variates. The idea of control variates, for European vanilla options, was first proposed by Andersen and Andreasen (2002) and further discussed by Cont and Tankov (2004). However, even with the help of control variates, the truncation bound for (10) will still retain some sensitivity to other factors such as the maturity of the option. Specifically, choosing a truncation bound that works well for a certain maturity will not be appropriate for another maturity; figure 9 illustrates this phenomenon. The sensitivity of the truncation bound is particularly severe for short maturities.

Similar to the seminal article of Abate and Whitt (1992), the new Laplace inversion algorithm of Iseger (2006) is a Fourier-based inversion method. As can be seen from the LHS of equation (8), it involves Laplace

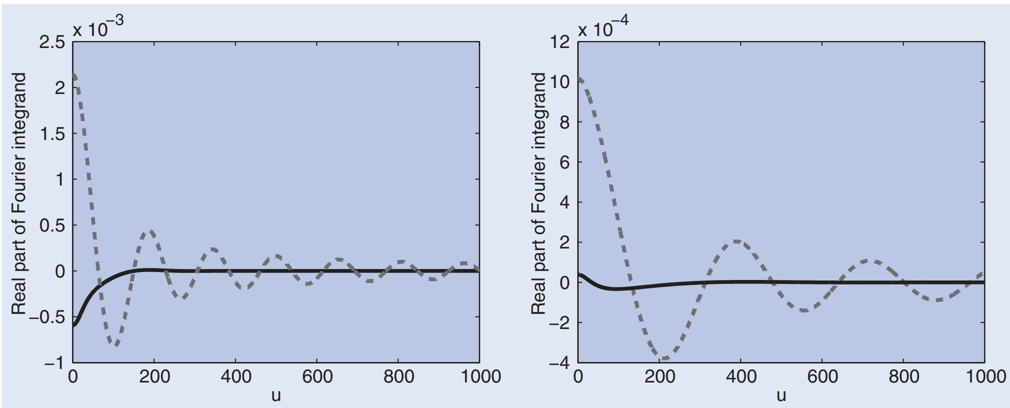

Figure 8. Real part of the Fourier integrand without control variates (- - - -) and with control variates (——) in the 3/2 model. Left: 6M maturity. Right: 3M maturity.

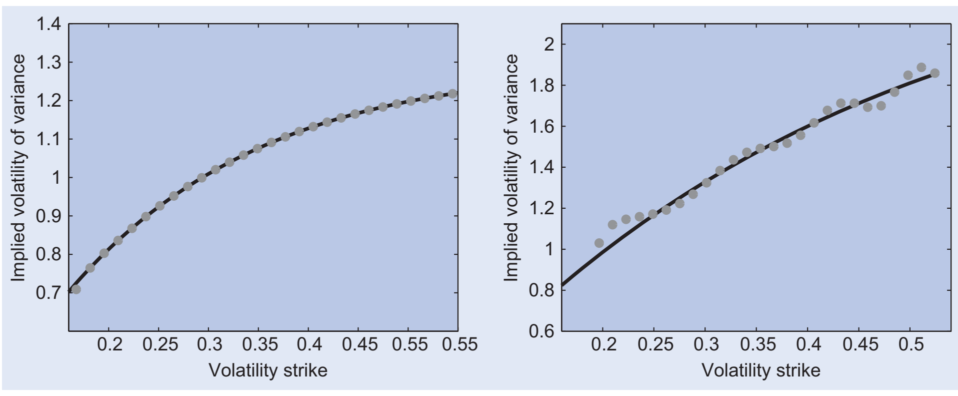

Figure 9. Left: 3M options on realized variance by GQ-FFT (——) and by standard Fourier inversion with Gamma control variates (●) in the 3/2 model. Right: Same for 1M maturity.

transform values on the fixed line $a+iu$, $u\in\mathbb{R}$; as mentioned above, this is the same as looking at the Fourier transform of the dampened call price $e^{-aK}\cdot 1_{K\geq 0}\cdot C(K)$. However, the key advantage over the standard Fourier methods is that it completely eliminates the need to perform any (semi-heuristic) truncations. It achieves this by the simple, but powerful, idea of constructing a Gaussian quadrature for the series of Laplace transform (or Fourier transform) values. Numerical tests for an extensive list of functions can be found in Iseger (2006). It provides conclusive evidence that the new algorithm is faster and more accurate than previously developed methods. In the calculations reported in this section, we considered both the rather mild (at least for equity markets) parameter set of Bakshi *et al.* (1997) (with a volatility-of-volatility $\epsilon=0.39$) as well as the more extreme parameter set (with a volatility-of-volatility $\epsilon=0.9288$) fitted to the July 31, 2009 volatility smile. For all maturities and both models, we considered very wide ranges of volatility strikes from 50 to 200% of the ATM volatility. Moreover, the well-behaved numerical results allowed us to differentiate twice the variance call prices to yield the full smooth density of realized variance in both models. In all cases, we found the new pricing method based on the Gaussian quadrature-fast Fourier transform (GQ-FFT) to be accurate and stable.

4. Hedge ratios for options on realized variance

The Laplace transform method developed in the previous section can also be applied to compute hedge ratios for options on realized variance. The natural hedging instruments for options on realized variance are their underlying variance swaps. Similar to options on stocks, we need to determine a delta, here with respect to variance swaps. As shown by Broadie and Jain (2008a), one can derive that the correct amount of delta, for a variance call of strike K, is given by

$$\Delta_{\mathrm{VS}}=\frac{(\partial/\partial v_0)C(K)}{(\partial/\partial v_0)C(0)},$$

where v_0 is the current value of the short variance process and $C(0)=E((1/T)\int_0^T v_t\,\mathrm{d}t)$ is the current fair variance swap rate for maturity T. The formula is intuitively clear: to hedge against the randomness in the short variance process, one needs to look at the ratio of the sensitivities of the two instruments—option on variance and variance swap—with respect to the value of the short variance. From the inversion equation (9) of the previous section, it can be seen that, in order to derive $(\partial/\partial v_0)C(K)$, we need to have the expressions for $(\partial/\partial v_0)\mathcal{L}(\lambda)$ in both models, where $\mathcal{L}(\lambda)$ is the Laplace transform of the annualized realized variance. From section 2, $\mathcal{L}(\lambda)$ is obtained from propositions 2.1 and 2.2 by setting $t=0$, $u=0$ and $\lambda=\lambda/T$.

From proposition 2.1, we obtain for the Heston model

$$\frac{\partial}{\partial v_0}\mathcal{L}(\lambda)=-b(0,T)\cdot\exp\left(a(0,T)-b(0,T)v_0\right),$$

with $a(0,T)$ and $b(0,T)$ as defined in proposition 2.1. Similarly, using proposition 2.2 and the property of the confluent hypergeometric function

$$\frac{\partial}{\partial z}M(\alpha,\gamma,z)=\frac{\alpha}{\gamma}M(\alpha+1,\gamma+1,z),$$

we obtain for the 3/2 model

$$\frac{\partial}{\partial v_0}\mathcal{L}(\lambda)=-\frac{\alpha z^{\alpha}}{v_0}\frac{\Gamma(\gamma-\alpha)}{\Gamma(\gamma)}\times\left[M(\alpha,\gamma,-z)-\frac{z}{\gamma}M(\alpha+1,\gamma+1,-z)\right],$$

with α and γ as defined in proposition 2.2 and

$$z=\frac{2}{\epsilon^2 y(0,T)}.$$

Using these results, we can apply the inversion tools developed previously to obtain the variance swap deltas for call options on realized variance at a sequence of strikes simultaneously. In figure 10 we show the results for the Heston and 3/2 models calibrated in section 2. As expected, we note that the behavior of the variance swap delta is similar to the delta of vanilla stock options. As we move from deep in the money calls to deep out of the money calls, the variance swap delta smoothly decreases from 1 to 0. Besides the six-month maturity, we also show, in figure 10(right), a short maturity of one

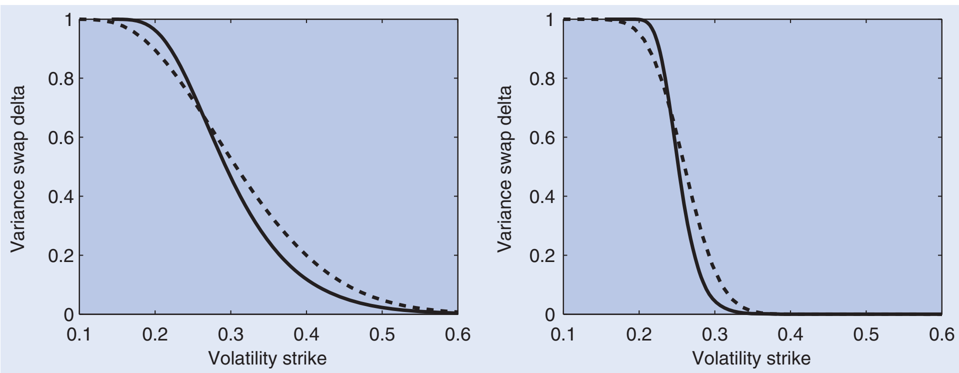

Figure 10. Variance swap delta for call options on realized variance with six months (left) and one week (right) to expiry as a function of strike expressed as a volatility. (——) 3/2 model. (- - - -) Heston model.

week and note that delta approaches the expected digital behavior near expiry.

5. Conclusion

We have developed a fast and robust method for determining prices and hedge ratios for options on realized variance applicable in any model where the Laplace transform of realized variance is available in closed form. The method was used to price options on realized variance in the 3/2 stochastic volatility model and in the Heston (1993) model. It has been shown that the 3/2 model offers several advantages for trading and risk managing volatility derivatives. Unlike the 3/2 model, the Heston model assigns significant weight to very low and vanishing volatility scenarios and is unable to produce extreme paths with very high volatility of volatility. Most importantly, the 3/2 model generates upward-sloping implied volatility of variance smiles—in agreement with the way variance options are traded in practice. Finally, we have shown that the transform methods can be efficiently used to obtain hedge ratios for options on realized variance.

References

Abate, J. and Whitt, W., The Fourier series method for inverting transforms of probability distributions. *Queuing Syst*., 1992, **10**, 5–88.

Ahn, D. and Gao, B., A parametric nonlinear model of term structure dynamics. *Rev. Financial Stud*., 1999, **12**, 721–762.

Aït-Sahalia, Y., Mykland, P. and Zhang, L., How often to sample a continuous-time process in the presence of market microstructure noise. *Rev. Financial Stud*., 2005, **18**(2), 351–416.

Albanese, C., Lo, H. and Mijatovic, A., Spectral methods for volatility derivatives. *Quant. Finance*, 2009, **9**(6), 663–692.

Andersen, L. and Andreasen, J., Volatile volatilities. *Risk*, 2002, **5**, 163–168.

Andreasen, J., Dynamite dynamics. In *Credit Derivatives: The Definitive Guide*, edited by J. Gregory, 2003 (Risk Publications: London).

Bakshi, G., Cao, C. and Chen, Z., Empirical performance of alternative option pricing models. *J. Finance*, 1997, **LII**(5).

Bakshi, G., Ju, N. and Yang, H., Estimation of continuous time models with an application to equity volatility. *J. Financial Econ*., 2006, **82**(1), 227–249.

Bergomi, L., Smile dynamics 2. *Risk Mag*., 2005, 67–73.

Bergomi, L., Smile dynamics 3. *Risk Mag*., 2008, 90–96.

Black, F. and Scholes, M., The pricing of options and corporate liabilities. *J. Polit. Econ*., 1973, **81**, 637–654.

Breeden, D. and Litzenberger, R., Prices of state contingent claims implicit in option prices. *J. Business*, 1978, **51**(6), 621–651.

Broadie, M. and Jain, A., Pricing and hedging volatility derivatives. *J. Deriv*., 2008a, **15**(3), 7–24.

Broadie, M. and Jain, A., The effect of jumps and discrete sampling on volatility and variance swaps. *Int. J. Theor. Appl. Finance*, 2008b, **11**(8), 761–797.

Carr, P., Geman, H., Madan, D. and Yor, M., Pricing options on realized variance. *Finance Stochast*., 2005, **9**(4), 453–475.

Carr, P. and Lee, R., Realized volatility and variance: Options via swaps. *Risk Mag*., 2007, **May**, 76–83.

Carr, P. and Madan, D., Option pricing and the fast Fourier transform. *J. Comput. Finance*, 1999, **2**(4), 61–73.

Carr, P. and Madan, D., Towards a theory of volatility trading. In *Volatility: New Estimation Techniques for Pricing Derivatives*, edited by R. Jarrow, pp. 417–427, 2002 (Risk Publications: London).

Carr, P. and Sun, J., A new approach for option pricing under stochastic volatility. *Rev. Deriv. Res*., 2007, **10**, 87–150.

Chesney, M. and Scott, L., Pricing European currency options: A comparison of the modified Black-Scholes model and a random variance model. *J. Financial Quant. Anal*., 1989, **24**, 267–284.

Cont, R. and Tankov, P., *Financial Modeling with Jump Processes*, 2004 (Chapman & Hall: London).

Cooley, J.W. and Tukey, J., An algorithm for the machine calculation of complex Fourier series. *Math. Comput*., 1965, **19**, 297–301.

Cox, J.C., Ingersoll, J.E. and Ross, S.A., A theory of the term structure of interest rates. *Econometrica*, 1985, **53**, 385–407.

Demeterfi, K., Derman, E., Kamal, M. and Zou, J., A guide to volatility and variance swaps. *J. Deriv*., 1999, **4**, 9–32.

Dubner, H. and Abate, J., Numerical inversion of Laplace transforms by relating them to the finite Fourier cosine transform. *J. ACM*, 1968, **15**, 115–123.

Duffie, D., Pan, J. and Singleton, K., Transform analysis and asset pricing for affine jump-diffusions. *Econometrica*, 2000, **68**, 1343–1376.

Dufresne, D., The integrated square-root process. Research Paper No. 90 University of Melbourne, 2001.

Eberlein, E. and Madan, D., Sato processes and the valuation of structured products. *Quant. Finance*, 2009, **9**(1), 27–42.

Friz, P. and Gatheral, J., Valuation of volatility derivatives as an inverse problem. *Quant. Finance*, 2005, **5**(6), 531–542.

Gatheral, J., *The Volatility Surface: A Practitioner's Guide*, 2006 (Wiley: New York).

Gatheral, J. and Oomen, R., Zero intelligence realized variance estimation. *Finance Stochast*, 2010, **14**(2), 249–283.

Heston, S., A closed-form solution for options with stochastic volatility with applications to bond and currency options. *Rev. Financial Stud*., 1993, **6**, 327–343.

Hull, J. and White, A., The pricing of options on assets with stochastic volatilities. *J. Finance*, 1987, **XLII**(2), 281–300.

Iseger, P., Numerical transform inversion using Gaussian quadrature. *Probab. Engng Inform. Sci*., 2006, **20**, 1–44.

Jones, C., The dynamics of stochastic volatility: Evidence from underlying and options markets. *J. Econometr*., 2003, **116**, 118–224.

Lewis, A., *Option Valuation Under Stochastic Volatility*, 2000 (Finance Press: Newport Beach, CA).

Medvedev, A. and Scaillet, O., Approximation and calibration of short-term implied volatilities under jump-diffusion stochastic volatility. *Rev. Financial Stud*., 2007, **20**, 427–459.

Merton, R., Option pricing when underlying stock returns are discontinuous. *J. Financial Econ*., 1976, **3**, 125–144.

Neuberger, A., The log contract. *J. Portfol. Mgmt*, 1994, **20**(2), 74–80.

Overhaus, M., *et al*., *Equity Hybrid Derivatives*, 2007 (Wiley: New York).

Schlögl, E. and Schlögl, L., A square root interest rate model fitting discrete initial term structure data. *Appl. Math. Finance*, 2000, **7**(3), 183–209.

Scott, L., Option pricing when the variance changes randomly: Theory, estimation and an application. *J. Financial Quant. Anal*., 1987, **22**, 419–438.

Sepp, A., Pricing options on realized variance in the Heston model with jumps in returns and volatility. *J. Comput. Finance*, 2008, **11**(4), 33–70.

Stehfest, H., Algorithm 368: Numerical inversion of Laplace transforms. *Commun. ACM*, 1970, **13**, 47–49.

Talbot, A., The accurate inversion of Laplace transforms. *J. Inst. Math. Applic*., 1979, **23**, 97–120.

Weeks, W.T., Numerical inversion of Laplace transforms using Laguerre functions. *J. ACM*, 1966, **13**, 419–426.

Appendix A: Proofs

Proof of proposition 2.1

Proof: We are in a special case of the general multi-factor affine framework introduced by Duffie *et al.* (2000). With $X_t = \log(S_t e^{(r-\delta)(T-t)})$ denoting the log forward process, we have

$$\mathrm{d}X_t = -\frac{v_t}{2}\,\mathrm{d}t + \sqrt{v_t}\,\mathrm{d}B_t,$$
$$\mathrm{d}v_t = k(\theta(t) - v_t)\mathrm{d}t + \epsilon\sqrt{v_t}\,\mathrm{d}W_t.$$

The state vector (X_t, v_t) is a two-dimensional affine process as defined by Duffie *et al.* (2000). Let

$$\psi(X_t, v_t, t) = E\left(e^{iuX_T - \lambda\int_t^T v_s\,\mathrm{d}s} \mid X_t, v_t\right)$$

denote the joint Fourier–Laplace transform of X_T and the de-annualized integrated variance $\int_t^T v_s\,\mathrm{d}s$. Observing that the process

$$e^{-\lambda\int_0^t v_s\,\mathrm{d}s}\cdot\psi(X_t, v_t, t) = E\left(e^{iuX_T - \lambda\int_0^T v_s\,\mathrm{d}s} \mid X_t, v_t\right)$$

is a martingale, an application of Ito's Lemma gives the following partial differential equation for $\psi(x, v, t)$:

$$\frac{1}{2}\epsilon^2 v\psi_{vv} + k(\theta(t) - v)\psi_v + \epsilon\rho v\psi_{xv} - \frac{1}{2}v\psi_x + \frac{1}{2}v\psi_{xx} - \lambda v\psi + \psi_t = 0,$$

with terminal condition

$$\psi(x, v, T) = e^{iux}.$$

Looking for a solution of the form

$$\psi(x, v, t) = \exp(iux + a(t, T) - b(t, T)v)$$

leads to the ODEs for $a(\cdot, T)$ and $b(\cdot, T)$:

$$b' = \frac{1}{2}\epsilon^2 b^2 + (k - i\epsilon\rho u)b - \left(\frac{1}{2}iu + \frac{1}{2}u^2 + \lambda\right),$$
$$a' = k\theta(t)b,$$

with terminal condition $a(T, T) = b(T, T) = 0$, and a' and b' denoting derivatives with respect to t. The complex-valued ODE for $b(\cdot, T)$ can be solved in closed form (Cox *et al.* 1985, Heston 1993). In our case, the solution for $b(\cdot, T)$ is

$$b(t, T) = \frac{(iu + u^2 + 2\lambda)(e^{\gamma(T-t)} - 1)}{(\gamma + k - i\epsilon\rho u)(e^{\gamma(T-t)} - 1) + 2\gamma},$$

with

$$\gamma = \sqrt{(k - i\epsilon\rho u)^2 + \epsilon^2(iu + u^2 + 2\lambda)}.$$

Once the function $b(\cdot, T)$ is known, the ODE for $a(\cdot, T)$ gives

$$a(t, T) = -\int_t^T k\theta(s)b(s, T)\mathrm{d}s.$$

□

Proof of lemma 3.2

Proof: Rewrite the limit as

$$\lim_{K\downarrow 0}\frac{C(K) - C(0)}{K} = \lim_{K\downarrow 0}\frac{E(V-K)_+ - E(V)}{K} = \lim_{K\downarrow 0} E\left(\frac{(V-K)_+ - V}{K}\right).$$

Since $V > 0$ a.s. we have

$$\lim_{K\downarrow 0}\frac{(V-K)_+ - V}{K} = \lim_{K\downarrow 0}\frac{V - K - V}{K} = -1, \quad \text{a.s.}$$

Using the obvious bound

$$\left|\frac{(V-K)_+ - V}{K}\right| \le 1,$$

we can apply the dominated convergence theorem to interchange the order of limit and expectation

$$\lim_{K\downarrow 0} E\left(\frac{(V-K)_+ - V}{K}\right) = E\left(\lim_{K\downarrow 0}\frac{(V-K)_+ - V}{K}\right) = E(-1) = -1.$$

□

Proof of lemma 3.3

Proof: This result follows readily by direct integration. For $V \sim$ Gamma (α, β), we have

$$\tilde{C}(K) = E(V-K)_+ = \int_K^\infty (x - K)\frac{1}{\Gamma(\alpha)\beta^\alpha}x^{\alpha-1}e^{-x/\beta}\,\mathrm{d}x.$$

Computing separately the integral corresponding to each term in parentheses, we obtain

$$\int_K^\infty \frac{1}{\Gamma(\alpha)\beta^\alpha}x^\alpha e^{-x/\beta}\,\mathrm{d}x = \int_K^\infty \frac{\alpha\beta}{\Gamma(\alpha+1)\beta^{\alpha+1}}x^\alpha e^{-x/\beta}\,\mathrm{d}x = \alpha\beta(1 - F(K; \alpha+1, \beta))$$

and

$$\int_K^\infty \frac{K}{\Gamma(\alpha)\beta^\alpha}x^{\alpha-1}e^{-x/\beta}\,\mathrm{d}x = K(1 - F(K; \alpha, \beta)),$$

where $F(\cdot, \alpha, \beta)$ is the CDF of the Gamma (α, β) distribution. □

Proof of proposition 3.4

Proof: In

$$h(y) = \int_0^y e^{-2/\epsilon^2 z}\cdot z^{2k/\epsilon^2}\cdot\int_z^\infty \frac{2}{\epsilon^2}\cdot e^{2/\epsilon^2 u}\cdot u^{(-2k/\epsilon^2)-2}\,\mathrm{d}u\,\mathrm{d}z,$$

denote $\alpha = 2/\epsilon^2 > 0$ and $\beta = -2k/\epsilon^2 < 0$ and rewrite the integral as

$$\alpha\int_0^y e^{-\alpha/z}z^{-\beta}\int_z^\infty e^{\alpha/u}u^{\beta-2}\,\mathrm{d}u\,\mathrm{d}z = \alpha\int_0^y e^{-\alpha/z}\int_z^\infty e^{\alpha/u}\left(\frac{z}{u}\right)^{-\beta}u^{-2}\,\mathrm{d}u\,\mathrm{d}z.$$

In the inner integral, making the change of variable $z/u = t$ we obtain

$$\int_z^\infty e^{\alpha/u}\left(\frac{z}{u}\right)^{-\beta} u^{-2}\,du = \frac{1}{z}\int_0^1 e^{\alpha t/z} t^{-\beta}\,dt.$$

Expanding $e^{\alpha t/z}$ in a series gives

$$\frac{1}{z}\int_0^1 \sum_{n=0}^\infty \frac{1}{n!}\left(\frac{\alpha}{z}\right)^n t^{n-\beta}\,dt = \sum_{n=0}^\infty \frac{1}{n!}\frac{\alpha^n}{z^{n+1}}\frac{1}{n-\beta+1},$$

where we have interchanged integration and summation as all terms are non-negative.

$$h(y) = \alpha\int_0^y e^{-\alpha/z}\sum_{n=0}^\infty \frac{1}{n!}\frac{\alpha^n}{z^{n+1}}\frac{1}{n-\beta+1}\,dz = \alpha\sum_{n=0}^\infty \frac{1}{n!(n-\beta+1)}\int_0^y \frac{\alpha^n e^{-\alpha/z}}{z^{n+1}}\,dz.$$

Making the change of variable $\alpha/z = t$, we obtain

$$\int_0^y \frac{\alpha^n e^{-\alpha/z}}{z^{n+1}}\,dz = \int_{\alpha/y}^\infty e^{-t}\cdot t^{n-1}\,dt.$$

For $n = 0$ we recognize the exponential integral function

$$E\left(\frac{\alpha}{y}\right) = \int_{\alpha/y}^\infty e^{-t}\cdot t^{-1}\,dt,$$

and for $n \geq 1$ we obtain the upper incomplete Gamma function, which satisfies

$$\int_{\alpha/y}^\infty e^{-t}\cdot t^{n-1}\,dt = (n-1)!\cdot e^{-\alpha/y}\cdot\sum_{k=0}^n \frac{(\alpha/y)^k}{k!} = (n-1)!\cdot F_{\alpha/y}(n),$$

where $F_\nu(\cdot)$ is the CDF of a Poisson random variable of parameter ν. Collecting the previous results, we obtain

$$h(y) = \alpha\cdot\left(\frac{E(\alpha/y)}{1-\beta} + \sum_{n=1}^\infty \frac{F_{\alpha/y}(n)}{n(n-\beta+1)}\right).$$

Uniform convergence follows from the bound

$$\sum_{n=k}^\infty \frac{F_{\alpha/y}(n)}{n(n-\beta+1)} < \sum_{n=k}^\infty \frac{1}{n(n-\beta+1)} < \sum_{n=k}^\infty \frac{1}{n(n+1)} = \frac{1}{k}.$$

□

Proof of lemma 3.5

Proof: The upper bound has been derived in the proof of proposition 3.4. If we let $m = \lceil -\beta \rceil$ (i.e. the smallest integer greater than or equal to $-\beta$), we can write

$$R_k = \sum_{n=k}^\infty \frac{F_{\alpha/y}(n)}{n(n-\beta+1)} > F_{\alpha/y}(k)\sum_{n=k}^\infty \frac{1}{n(n-\beta+1)} \geq \frac{F_{\alpha/y}(k)}{m+1}\sum_{n=k}^\infty \frac{m+1}{n(n+m+1)} = \frac{F_{\alpha/y}(k)}{m+1}\left(\frac{1}{k}+\frac{1}{k+1}+\cdots+\frac{1}{k+m}\right).$$

Let $\bar{R}$ denote the mid-point between the two bounds, i.e.

$$\bar{R} = \frac{1}{2}\left(\frac{1}{k} + \frac{F_{\alpha/y}(k)}{m+1}\left(\frac{1}{k}+\frac{1}{k+1}+\cdots+\frac{1}{k+m}\right)\right),$$

and let $p = F_{\alpha/y}(k)$. We then have that $|R_k - \bar{R}|$ must be less than or equal to half the difference between the two bounds, i.e.

$$|R_k - \bar{R}| \leq \frac{1}{2}\left(\frac{1}{k} - \frac{p}{m+1}\left(\frac{1}{k}+\frac{1}{k+1}+\cdots+\frac{1}{k+m}\right)\right) = \frac{1}{2(m+1)}\sum_{j=0}^m \frac{j+(1-p)k}{k(k+j)} < \frac{1}{2k^2(m+1)}\left(\frac{m(m+1)}{2} + (1-p)k(m+1)\right) = \frac{m}{4k^2} + \frac{1-p}{2k}.$$

Observing that

$$1 - p = e^{-\alpha/y}\cdot\sum_{n=k+1}^\infty \frac{(\alpha/y)^n}{n!} = e^{-\alpha/y}\cdot\sum_{n=k+1}^\infty \frac{(\alpha/y)(\alpha/y)^{n-1}}{n\cdot(n-1)!} < \frac{\alpha/y}{k}e^{-\alpha/y}\cdot\sum_{n=k}^\infty \frac{(\alpha/y)^n}{n!} < \frac{\alpha/y}{k},$$

we finally obtain

$$|R_k - \bar{R}| < \frac{m + 2(\alpha/y)}{4k^2}.$$

□

Proof of lemma 3.6

Proof: Bounded variation follows immediately by observing that $C(K) = E(V-K)_+$ is a monotone decreasing function of K. Next we check that $C(K) \in L^1[0,\infty)$, i.e.

$$\int_0^\infty C(K)dK = \int_0^\infty E(V-K)_+\,dK < \infty.$$

Since the integrand is positive, we can apply Fubini to change the order of integration and expectation:

$$\int_0^\infty E(V-K)_+\,dK = E\left(\int_0^\infty (V-K)_+\,dK\right) = E\left(\int_0^V V - K\,dK\right) = E\left(\frac{V^2}{2}\right) < \infty.$$